

## 552 Supplementary Information

553

### 554 1. Inference of ECNs from longitudinal data

555

556 We consider that abundance of  $O$  bacterial operational taxonomic units (OTUs) are measured  
557 over a period of  $T$  days in  $S$  subjects. We model the read counts  $n_{os}(t)$  of OTUs " $o$ " on any given  
558 day  $t$  in subject  $s$  as a multinomial distribution:

$$559 \quad p(\{n_{os}(t)\}) = \frac{N_s(t)!}{\prod_o n_{os}(t)!} \prod_o q_{os}(t)^{n_{os}(t)} \quad (S1)$$

560 where  $N_s(t) = \sum_o n_{os}(t)$  is the total read count on a given day and  $q_{os}(t)$  are the underlying  
561 propensities for individual OTUs. We model these propensities using the exponential Gibbs-  
562 Boltzmann distribution which allows us to capture large variations in OTU abundances<sup>33</sup>

$$563 \quad q_{os}(t) = \frac{1}{\Omega_{st}} \exp\left(-\sum_{k=1}^K z_k(t)\theta_{kos}\right) \quad (S2)$$

564 where  $z_k(t)$  are time-specific latents that are shared by all OTUs and subjects, and  $\theta_{kos}$  are OTU-  
565 and subject-specific loadings that are shared across all time points. The number  $K$  of  
566 latents/loadings is chosen such that  $K \ll O, T$  thereby achieving a lower dimensional description  
567 of the time series data. We obtain the  $z$ s and the  $\theta$ s using the maximum likelihood approach.

568

569 To that end, we write down the log-likelihood of the data:

$$570 \quad L = \text{const.} + \sum_{t,o,s} n_{os}(t) \log q_{os}(t). \quad (S3)$$

571 The constant term of the likelihood does not depend on the parameters and can thus be omitted  
572 in likelihood maximization. Simplifying using Eq. S1 and S2, we have

$$573 \quad L = -\sum_{t,o,s,k} N_s(t) x_{os}(t) z_k(t) \theta_{kos} - \sum_{t,s} \log \Omega_{st} \quad (S4)$$

574 Here  $x_{os}(t) = n_{os}(t)/N_s(t)$  is the relative abundance of OTU  $o$  at time  $t$ . We obtain the  
575 gradients

$$576 \quad \frac{\partial L}{\partial z_k(t)} = -\sum_{o,s} N_s(t) (x_{os}(t) - q_{os}(t)) \theta_{kos} \quad \text{and} \quad (S5)$$

$$577 \quad \frac{\partial L}{\partial \theta_{kos}} = -\sum_t N_s(t) z_k(t) (x_{os}(t) - q_{os}(t)) \quad (S6)$$

578 We use gradient ascent algorithm to find the latents and the loadings that maximize the  
579 likelihood.

580

581 For a given  $K$ , using the microbiome data  $x_{os}(t)$  and starting from random initialization, we first  
582 simultaneously infer the latents  $z_k(t)$  and the features  $\Theta_{kos}$ . We observe that the  $T \times K$  matrix

583  $\mathbf{z}$  of latents can be multiplied by an invertible matrix  $\mathbf{B}$  ( $\mathbf{z} \rightarrow \mathbf{zB}$ ) and the corresponding matrix  
584  $K \times O \times S$  matrix of features can be multiplied by the inverse  $\mathbf{B}^{-1}$  ( $\mathbf{\Theta} \rightarrow \mathbf{B}^{-1}\mathbf{\Theta}$ ) and the  
585 abundance predictions from the model do not change. Therefore, we use the Gram-Schmidt  
586 procedure to orthogonalize the matrix of latents such that  $\mathbf{z} \rightarrow \mathbf{z}'$  where  $\mathbf{z}'^T \mathbf{z}' = \mathbf{I}_K$  is an identity  
587 matrix. For any matrix of latents  $\mathbf{z}$ , the matrix multiplier  $\mathbf{B}$  that leads to the orthonormal  
588 transformation can be found by solving the equation  $\mathbf{B}^T(\mathbf{z}^T \mathbf{z})\mathbf{B} = \mathbf{I}_K$ . Once  $\mathbf{B}$  is identified, we  
589 also transform the  $\mathbf{\Theta}$  matrix ( $\mathbf{\Theta} \rightarrow \mathbf{\Theta}' = \mathbf{B}^{-1}\mathbf{\Theta}$ ). At the end of this procedure, we end up with  
590 orthonormal latents  $\mathbf{z}'$  and corresponding features  $\mathbf{\Theta}'$  that correspond to the same abundances  
591 as  $\mathbf{z}$  and  $\mathbf{\Theta}$ . For the sake of simplicity of notation, we drop the primes.

592

593 Next, we model the dynamics of the orthonormal latents using a linear dynamical system:

$$594 \quad z_k(t) = \sum_{k'} A_{kk'} z_{k'}(t) + u_k + \eta_k(t) \quad (S7)$$

595 where we assume that  $A_{kk'} = A_{k'k}$ , and  $\eta_k(t)$  are Gaussian distributed uncorrelated noise  
596 vectors:  $\langle \eta_k(t_1) \eta_{k'}(t_2) \rangle = \delta_{12} \delta_{kk'}$  where  $\delta_{ab}$  is the Kronecker delta function. Our task is to find  
597 the interaction matrix  $\mathbf{A}$  and the vector  $\mathbf{u}$  that fits this model. We achieve this using squared error  
598 minimization. We write

$$599 \quad E(\mathbf{A}, \mathbf{u}) = \sum_t (z_k(t) - z_{k,pred}(t))^2 \quad (S7)$$

600 where  $z_k(t)$  is the inferred latent and  $z_{k,pred}(t)$  is the corresponding prediction using  $z_k(t-1)$   
601 and Eq. S7. We restrict the summation only over time points  $t$  such that measurements are  
602 available for time points  $t$  and  $t-1$ . The squared error is minimized using a simulated annealing  
603 approach. Once the matrix  $\mathbf{A}$  is identified, we transform the orthonormal latents  $z_k(t)$  into  
604 ecological normal modes  $y_k(t)$  as described in the manuscript.

605

606 The scripts for obtaining ECNs  $\mathbf{y}$  and corresponding loadings  $\mathbf{\Phi}$  from read count data can be  
607 found at: <https://github.com/mayar-shahin/EMBED>.

608

## 609 **2. Generating *in silico* data**

610 **Out of Phase Sinusoids.** We generated 40 OTU abundances for 30 time points. The un-  
611 normalized abundances of 20 OTUs followed sinusoidal oscillation:  $X(t) = A_1(B_1 \sin(0.5t) + 1)$   
612 and the un-normalized abundances of the other 20 OTUs followed phase-shifted oscillation with  
613 the same frequency  $X(t) = A_1(B_1 \cos(0.5t) + 1)$ .  $A_s$  and  $B_s$  are uniform random numbers  
614 between 0 and 1. We normalize the generated abundances to produce the underlying probability  
615 distribution of the data. We used multinomial sampling with a sequencing depth of 25000 to  
616 generate relative OTU abundances on each day (SI Fig. 1, panels A and B).

617

618 **Exponentials and Sinusoids.** We generated 40 OTU abundances for 30 time points. 20 OTUs  
619 followed an exponential decay  $X(t) = 10A_1 \exp(-0.1t)$ , 10 OTUs oscillated according to  
620  $X(t) = A_2(B_2 \sin(0.5t) + 1)$  and 10 OTUs oscillated with double the frequency  $X(t) =$   
621  $A_3(B_3 \sin(t) + 1)$ . As above,  $A$ s and  $B$ s are uniform random numbers between 0 and 1. We  
622 sampled the abundances using the multinomial distribution as above (SI Fig. 1, panels C and D).

623  
624 **Sum of Sinusoids.** We generated 40 OTU abundances for 30 time points. 20 OTUs followed a  
625 single high frequency oscillation  $X(t) = A_1(B_1 \cos(1.5t) + 1)$ . The remaining OTU abundances  
626 were generated by the addition of two different sinusoids:  $X(t) = A_2(B_2 \sin(0.5t) +$   
627  $B_3 \sin(t) + 1)$ . As above,  $A$ s and  $B$ s are uniform random numbers between 0 and 1. We sampled  
628 the abundances using the multinomial distribution as above (SI Fig. 1, panels E and F).

### 629 **3. Obtaining the microbiome time series from sequencing data**

631 **Murine gut microbiome response to oscillating diet.** We downloaded the microbiome  
632 abundance time series data on mice fed an alternating diet of high fat high sugar chow (HFHS)  
633 and low-fat plant polysaccharide chow (LFPP) from Carmody et al.<sup>25</sup> as described previously<sup>14</sup>.  
634 Each mouse that was subjected to an oscillatory diet was treated separately. Based on our  
635 previous work on technical noise in 16s measurements, we only analyzed OTUs with mean  
636 abundances  $> 0.1\%$ <sup>13</sup> averaged across all time points and mice. On every day, the abundances of  
637 the rest of the OTUs were lumped together in a single meta-species.

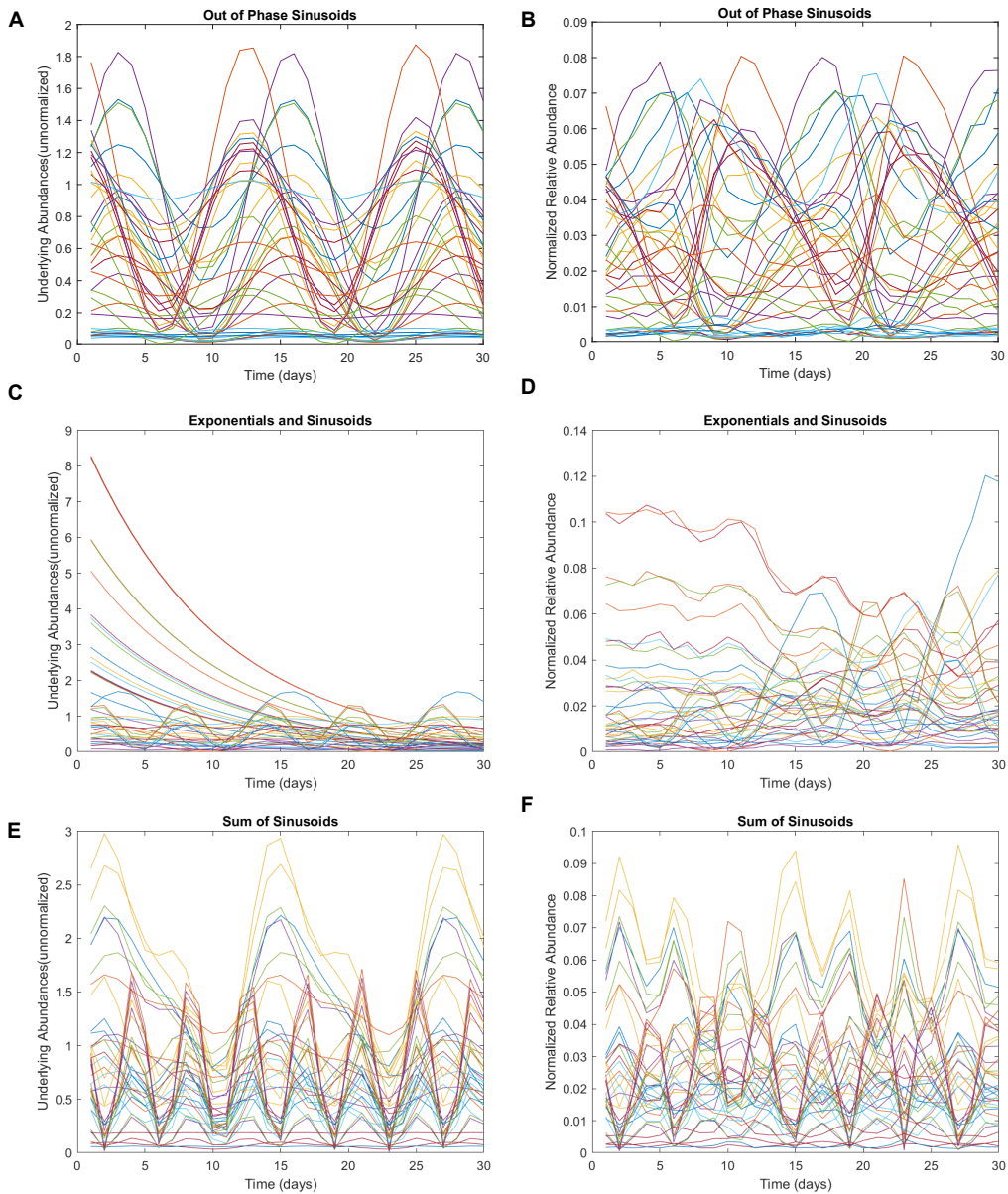
638  
639 **Murine gut microbiome response to antibiotics.** We downloaded microbiome abundance data  
640 from Ng et al.<sup>10</sup>. We focused on the data where mice were administered the antibiotic  
641 ciprofloxacin. Out of the 10 cages in which the mice were housed, we omitted data from cages  
642 2, 4, 5, and 8 where many time points were missing. As above, we analyzed OTUs with mean  
643 abundance  $> 0.1\%$  and combined the rest of the OTUs in a meta-species.

### 644 **4. Performing CLR and SSVD on 4 data sets**

646 We downloaded 4 publicly available data sets from 4 different studies<sup>10-12,25</sup>. Each data set  
647 comprised microbiome abundance tables for multiple subjects, see SI Table 1. We use the  
648 package released by Martino et al.<sup>32</sup> (<https://github.com/biocore/gemelli>) to perform Robust  
649 Centered-Log Ratio transform (CLR) on the abundances followed by sparse singular value  
650 decomposition. To test how well the dimensionality reduced version capture the data, we  
651 calculate an approximate reconstruction of the abundance time series using the first  $K$  singular  
652 values. As suggested by Martino et al.<sup>31</sup>, the resulting approximation was re-exponentiated and  
653 then normalized. We Then calculated the KL-divergence with the true abundances.

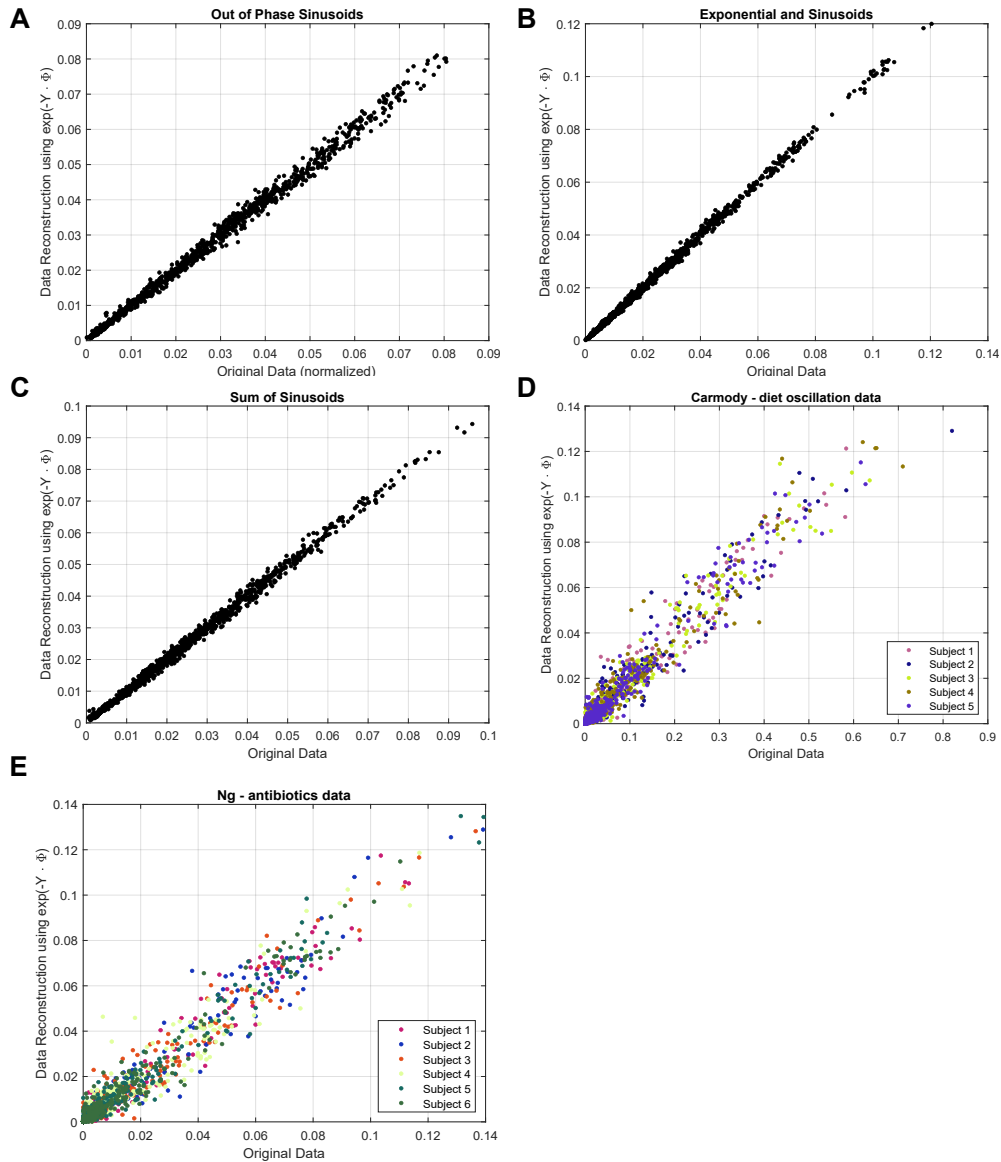
654  
655

656 **Supplementary Figures**  
657



658  
659 **Supplementary Figure 1.** Collective abundance variation of bacterial species in *in silico* data sets  
660 representing out of phase oscillations (A and B), exponential decays and oscillations (C and D), and sum  
661 of sinusoids (E and F).

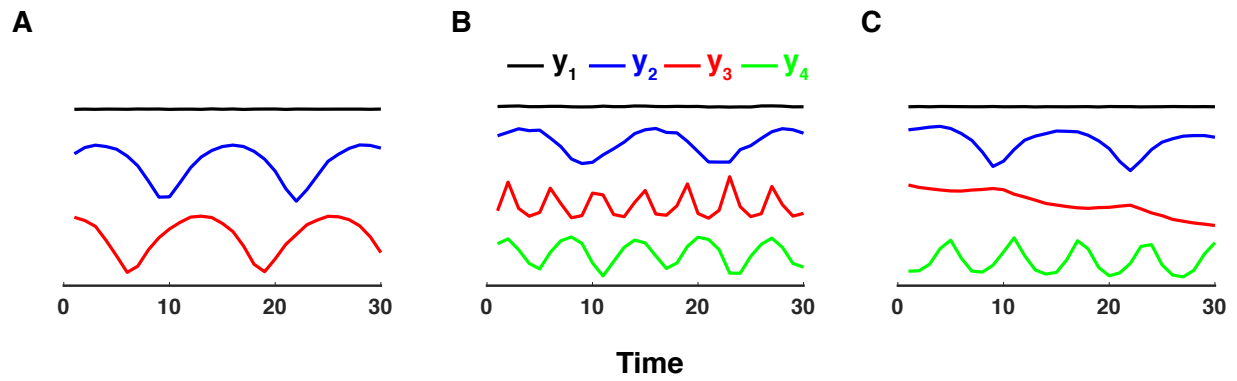
662  
663  
664  
665  
666



667  
 668 **Supplementary Figure 2.** EMBED-based reconstruction of time series (y axis) compared to the microbiome  
 669 time series data (x-axis) for the three *in silico* data sets (A, B, and C) and the two experimental data sets  
 670 (D and E) considered in this study.

671  
 672  
 673  
 674  
 675  
 676  
 677  
 678  
 679

680



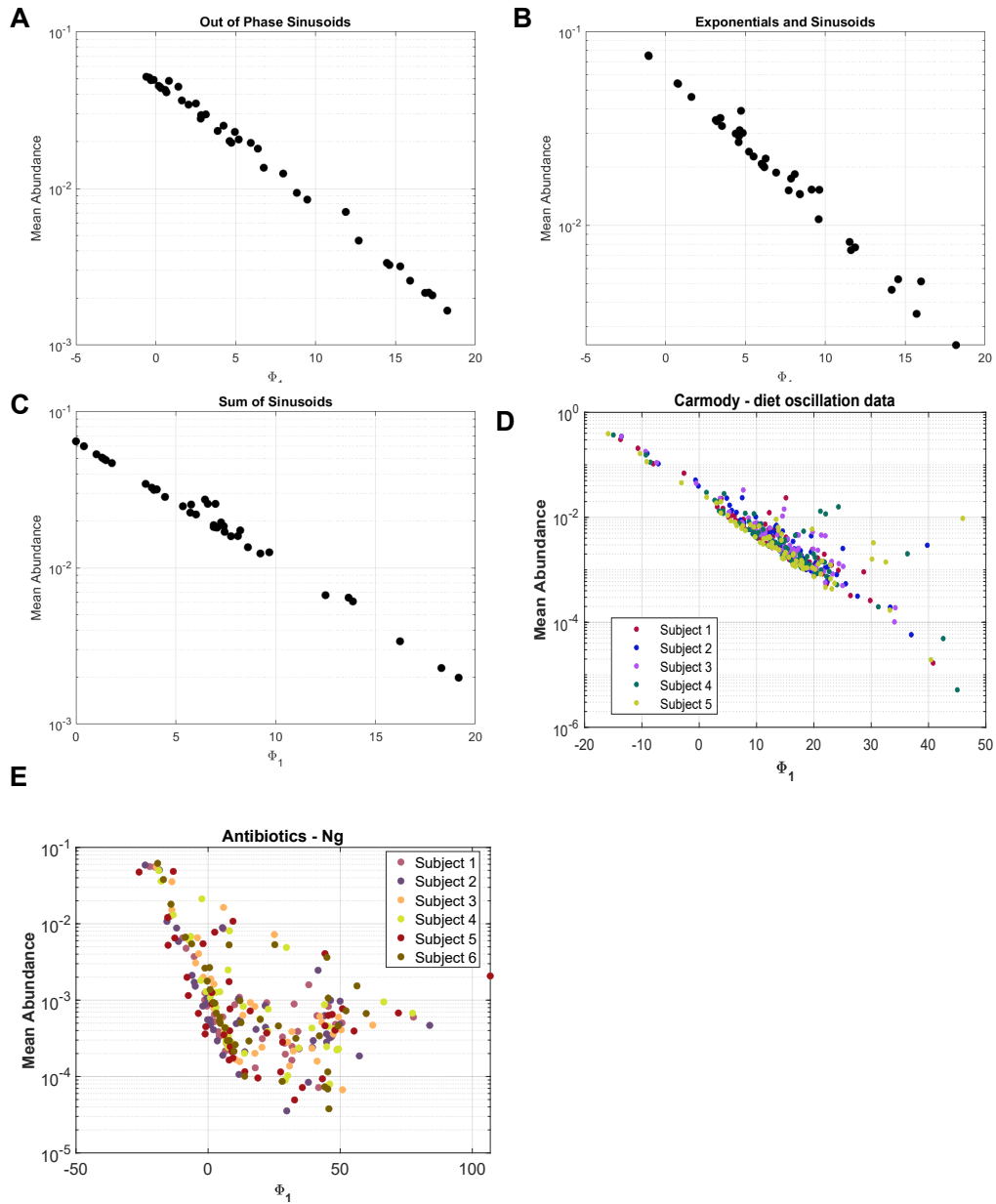
681

682 **Supplementary Figure 3.** EMBED-based inference of ecological normal modes for the three in silico data

683 sets. A: out of frequency oscillations, B: sum of sinusoids, and C: exponential decay and sinusoids

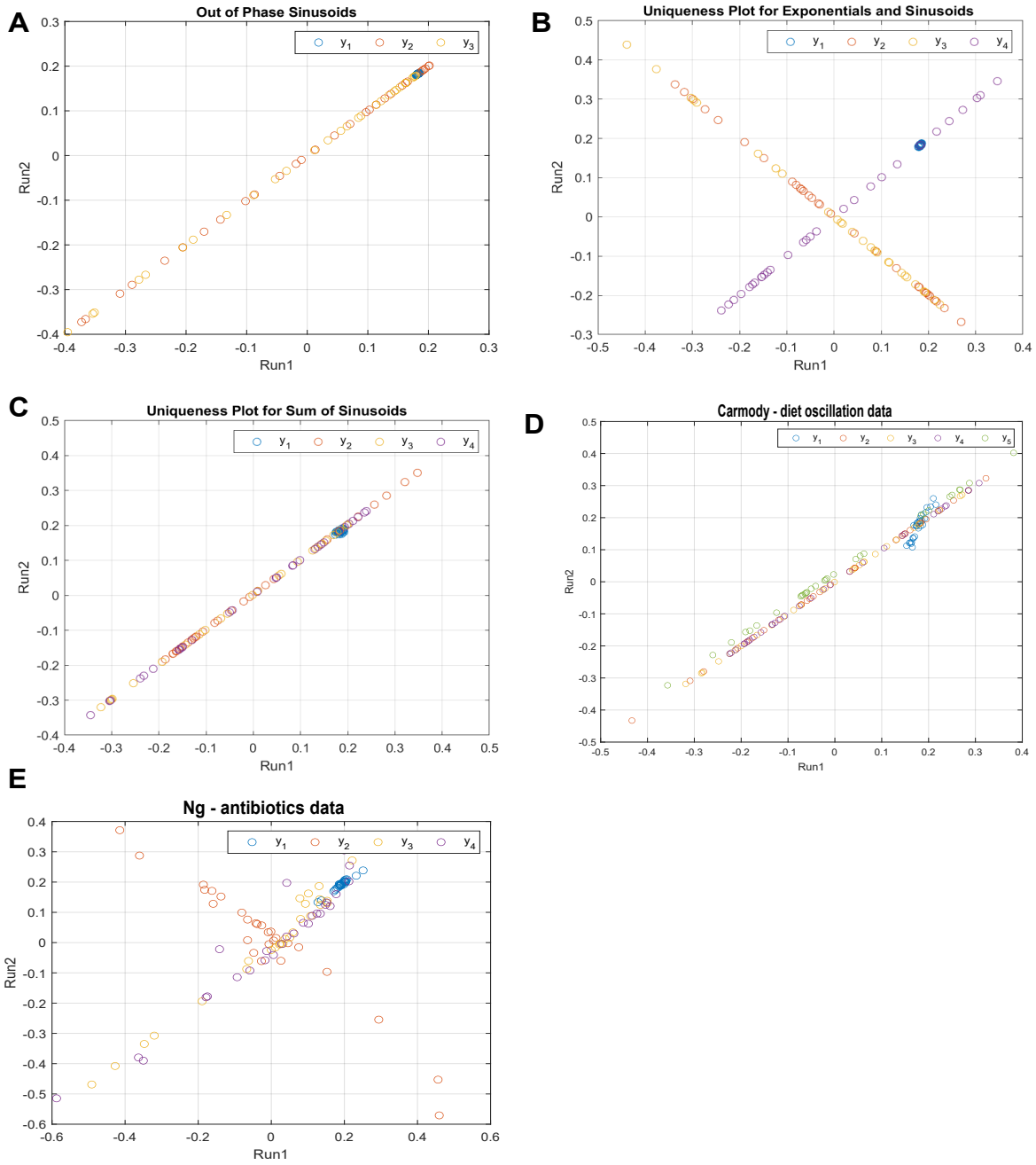
684

685



686  
 687 **Supplementary Figure 4.** Correlation between mean abundance of OTUs and their weight in the first  
 688 loading  $\Phi_1$  for the *in silico* data sets (A, B, and C) and the two experimental data sets (D and E) considered  
 689 in this study.

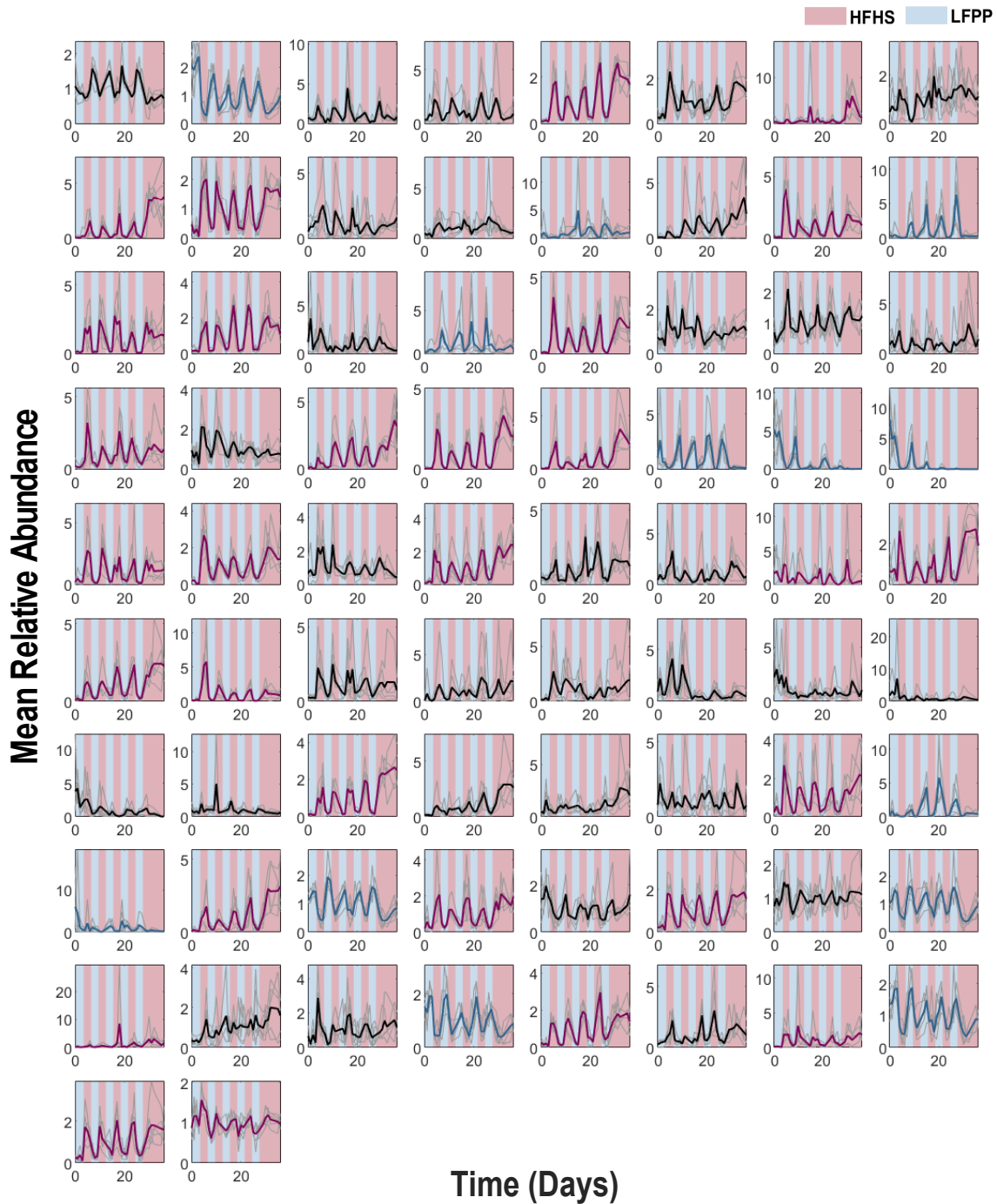
690  
 691  
 692  
 693  
 694  
 695



696  
 697  
 698  
 699  
 700  
 701  
 702  
 703  
 704

**Supplementary Figure 5.** Correlation plot showing that the ecological normal modes (ECNs) inferred using EMBED are unique (up to a sign). The x- and the y-axis represent the ECNs inferred in two independent runs.





706

707 **Supplementary Figure 6.** Abundance time series of individual OTUs in the diet oscillation study. The gray

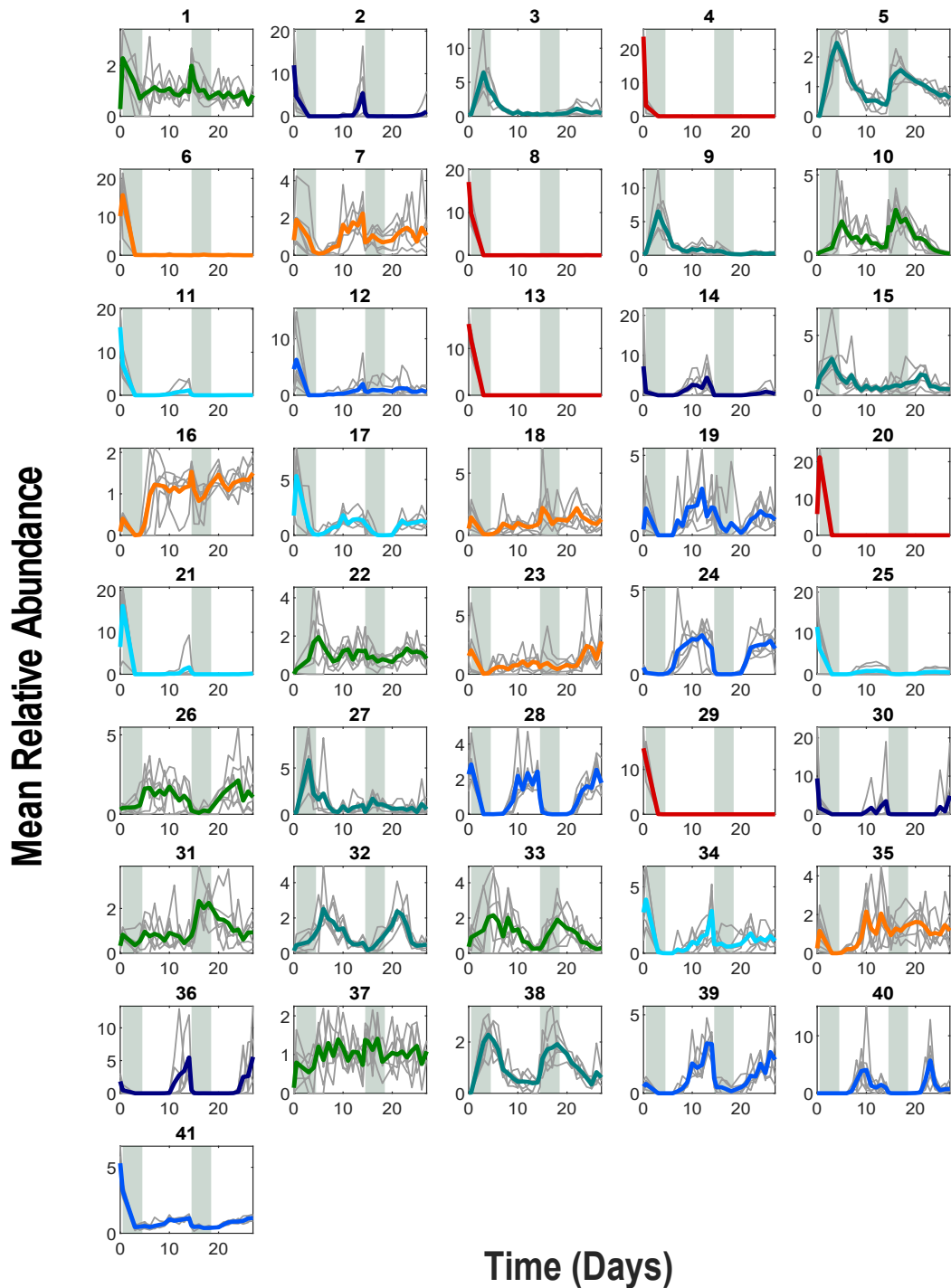
708 lines represent abundances in individual subjects. The dark lines represent averages over subjects. The

709 colors represent the cluster identities in main text Figure 2. HFHS: High Fat High Sugar diet and LFPP: Low

710 Fat Plat Polysaccharide diet.

711

712



713  
 714 **Supplementary Figure 7.** Abundance time series of individual OTUs in the antibiotics-treatment study.  
 715 The gray lines represent abundances in individual subjects. The dark lines represent averages over  
 716 subjects. The colors represent the cluster identities in main text Figure 3. The gray bars represent the  
 717 duration of time when the antibiotic was administered.

718  
 719